



Aircraft Takeoff and Landing Weight Estimation from Surveillance Data

Sandro Salgueiro*, R. John Hansman[†]
Massachusetts Institute of Technology, Cambridge, MA, 02139

Jacqueline Huynh[‡]
University of California Irvine, Irvine, CA, 92697

Aircraft weight estimation is a common problem facing researchers working with aircraft surveillance data such as ADS-B and ASDE-X data. Although knowledge of an aircraft's weight and thrust is required for many types of analyses, such as those evaluating aircraft acoustic noise, fuel burn and emissions, these parameters are typically not available from surveillance sources. Instead, researchers generally only have access to basic aircraft states: position, airspeed, and altitude. Therefore, methods to estimate the weight of aircraft from this type of data become necessary in situations in which aircraft performance is a key component of the analysis. This paper introduces two weight estimation models: one for estimation of aircraft takeoff weight from departure data, and another for estimation of aircraft landing weight from arrival data. The models are mathematically simple but grounded on knowledge of airline operations and in particular on the operation of modern aircraft Flight Management Systems (FMS). The landing weight estimation model proposed is shown to have a mean absolute error of 2.65% MTOW and a standard deviation of 3.36% MTOW when validated using Flight Data Recorder (FDR) data from 240 Airbus A320 flights. Similarly, the proposed takeoff weight estimation model is shown to have a mean absolute error of 2.66% MTOW and a standard deviation of 3.33% MTOW when applied to the same FDR dataset.

I. Nomenclature

<i>ADS-B</i>	=	Automatic Dependent Surveillance-Broadcast
<i>ASDE-X</i>	=	Airport Surface Detection Equipment, Model X
<i>ASR</i>	=	Airport Surveillance Radar
<i>BADA4</i>	=	Base of Aircraft Data 4
<i>BOS</i>	=	Boston Logan Airport
<i>MLW</i>	=	Maximum Landing Weight
<i>MTOW</i>	=	Maximum Takeoff Weight
<i>FMS</i>	=	Flight Management System
<i>IAS</i>	=	Indicated Airspeed
<i>NM</i>	=	Nautical Mile
<i>KIAS</i>	=	Indicated Airspeed in Knots
<i>kt</i>	=	Knots (Nautical Miles per Hour)
<i>TAS</i>	=	True Airspeed
<i>V₂</i>	=	Takeoff Safety Speed
<i>RWY</i>	=	Runway
<i>V_{APP}</i>	=	Aircraft Approach Speed
<i>V_{REF}</i>	=	Aircraft Approach Reference Speed
<i>V_s</i>	=	Aircraft Stall Speed
<i>V_{s1g}</i>	=	Aircraft Stall Speed at 1g Load Factor

*Graduate Student, Department of Aeronautics and Astronautics, 77 Massachusetts Avenue, Cambridge, MA 02139, sandrosr@mit.edu.

[†]Professor, Department of Aeronautics and Astronautics, 77 Massachusetts Avenue, Cambridge, MA 02139 rjhans@mit.edu.

[‡]Assistant Professor, Department of Mechanical and Aerospace Engineering, 4200 Engineering Gateway, Irvine, CA 92697, huynhjl@uci.edu.

II. Introduction

Aircraft surveillance systems (e.g. ASDE-X, ADS-B, ASR) are a common source of data in studies of aircraft operations, such as those attempting to measure airspace utilization, airport throughput, environmental impacts of aviation [1], and other system metrics. Due to the scale of surveillance data collection in the National Airspace System (NAS) and the relative ease with which this data can be acquired for research, these sources are used widely by research groups when more comprehensive data sources such as aircraft Flight Data Recorders (FDR) are either difficult to obtain or altogether unavailable.

However, due to surveillance systems typically only recording basic aircraft states, namely position, groundspeed and altitude, the data typically lack the full set of parameters (e.g. weight and thrust) required to fully characterize aircraft performance. In particular, analyses of fuel burn and aircraft acoustic noise rely on knowledge of the aircraft weight [2], which is not available from the surveillance data alone. While statistical models to estimate aircraft takeoff weight exist in literature [3], this paper proposes a simple and robust approach grounded on actual airline standard operating procedures and modern Flight Management System (FMS) logic. For example, by understanding how modern Flight Management Systems (FMS) compute approach speeds on final approach, we can estimate an aircraft's landing weight from its observed airspeed. The paper introduces methods for computing the takeoff weight of departing aircraft, as well as the landing weight of landing aircraft. Each method presented is validated using FDR data recorded during real airline operations, with the FDR providing aircraft weight.

III. Preparing Surveillance Data for Weight Estimation

The models derived in this paper rely primarily on airspeed and altitude measurements recorded by surveillance sensors to estimate aircraft takeoff and landing weights. For landing weight estimation, a model correlating aircraft approach speed to landing weight is proposed, while a correlation of specific energy (i.e. climb performance) and takeoff weight is proposed as the method to estimate takeoff weight.

While surveillance sources such as ASDE-X have enough resolution to provide an accurate reading of aircraft position and altitude, noise in measurements can sometimes be large enough to impact calculations related to aircraft performance. In particular, groundspeed measurements are commonly derived by differentiating aircraft position, which makes them especially susceptible to noise errors. As a result, depending on the quality of the data being utilized, it may be beneficial to filter the data before applying the models described in this paper. This step can help remove non-physical high-frequency behaviors that may ultimately lead to errors in weight estimation. Since this paper focuses on takeoff and landing weight estimation, filtering is only required in the initial climb and approach phases of flight.

A. Filtering on Initial Climb

The initial climb of large transport aircraft can typically be segmented into four basic phases: 1) rotation on the runway, 2) climb-out at a speed of V_2 plus some margin, 3) acceleration and flap retraction, 4) climb at constant airspeed. The acceleration phase can be further divided into acceleration with flaps down and acceleration with flaps retracted. Figure 1 illustrates conceptually how True Airspeed (TAS) and altitude are expected to change in each of these phases.

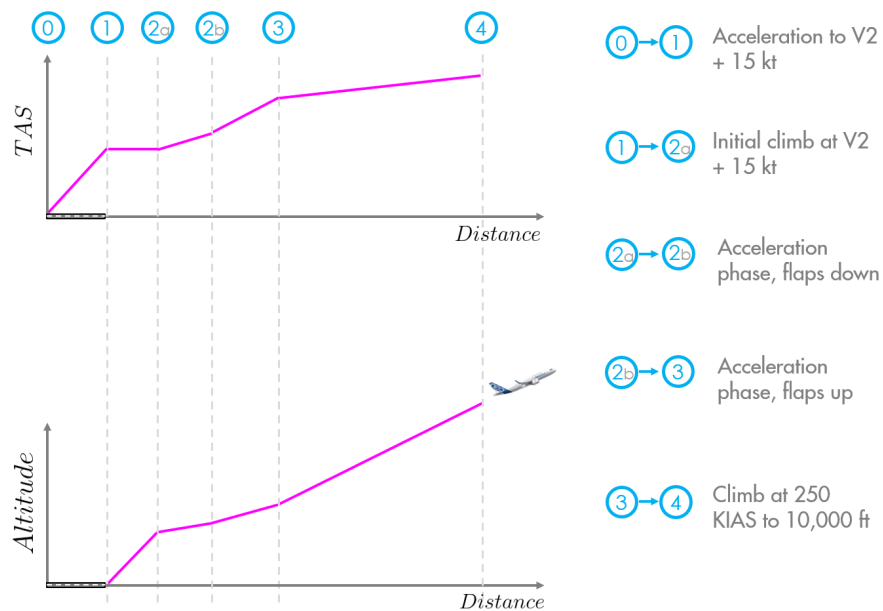


Fig. 1 Illustration of how the initial climb phase can be segmented into piecewise linear segments.

Because this behavior structure is largely repeatable among large commercial jets, and because aircraft speed and altitude change relatively linearly in each of the phases described, this structure can be enforced as a simple multi-piece linear fit for the flight data. Figure 2 illustrates how this can be applied to surveillance data as a low-pass filter alternative.

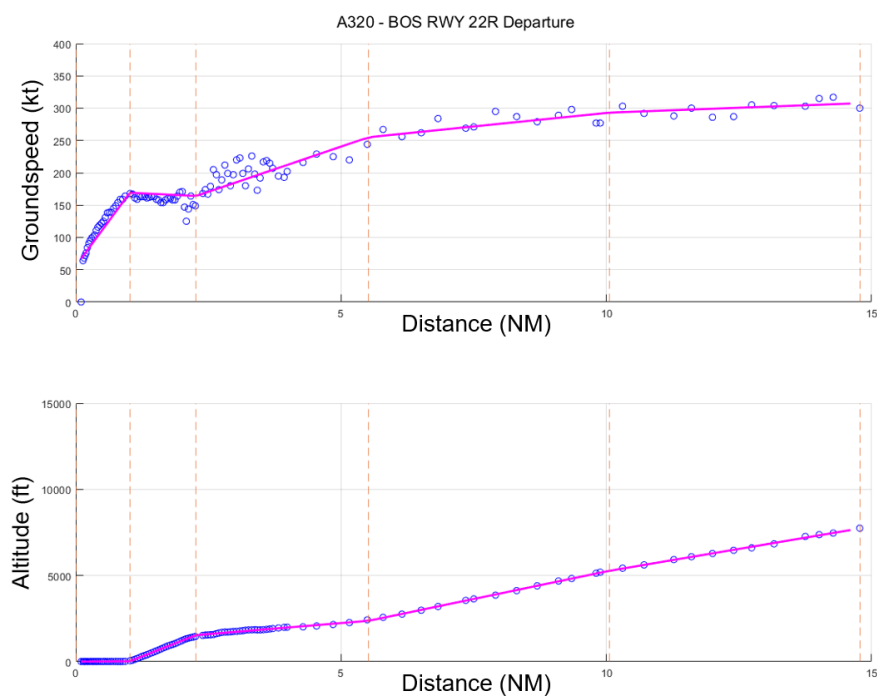


Fig. 2 Example of a five-piece linear fit applied to the ASDE-X data (groundspeed and altitude) of an Airbus A320 departure at Boston Logan Airport.

B. Filtering on Final Approach

While the altitude profiles of aircraft established on a final approach are very consistent due to the common 3-degree glideslope, deceleration (i.e. airspeed) profiles can still show considerable variation from aircraft to aircraft. Deceleration to final approach speed is a dynamic process, often affected by winds, pilot preference, flight procedure constraints, air traffic control technique, and traffic levels at the airport. As such, a consistent segmentation of the airspeed profile on final approach is not practical. While a multi-piece linear fit can be applied to the final approach as was done for the initial climb, no clear choice exists for the optimal number of segments. In filtering ASDE-X data available for Boston Logan Airport, it was found that a three- or four-piece segmentation of the airspeed and altitude profiles worked best for the final approach, although other filtering techniques may be equally effective in removing high-frequency noise. Figure 3 shows an example of a multi-piece linear fit applied to an ASDE-X approach at Boston Logan Airport.

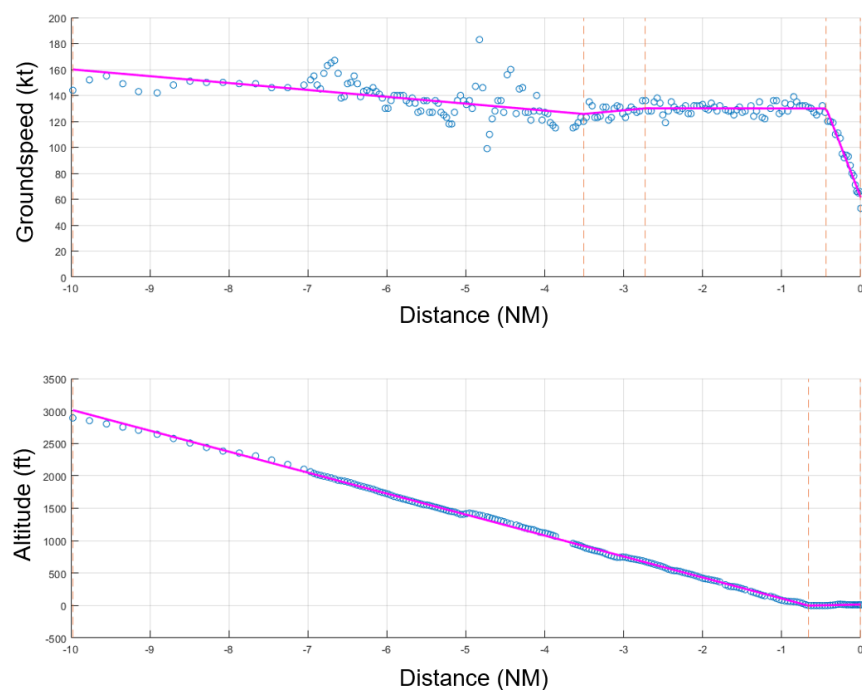


Fig. 3 Example of a four-piece linear fit applied to the ASDE-X groundspeed data of an Airbus A320 approach at Boston Logan Airport. Note that a simpler two-piece fit was used for the altitude data.

IV. Landing Weight Estimation

In this section, a model is derived for estimating the landing weight of an aircraft based on airspeed measurements from the final approach. To better expand on the method of estimation, a discussion of aircraft landing performance is warranted.

Most modern commercial aircraft are equipped with Flight Management Systems (FMS) that perform an automatic calculation of V_{REF} , the approach reference speed. V_{REF} can be calculated in two ways depending on how the aircraft's manufacturer demonstrated stall speed during certification flight test [4]. Most modern aircraft in operation today publish stall speed as V_{s1g} . In this scenario, V_{REF} is computed as:

$$V_{REF} = 1.23 \times V_{s1g}$$

Other aircraft, particularly older aircraft, publish stall speed as V_s , which is demonstrated using an older flight test technique. When V_s is published, V_{REF} is computed as:

$$V_{REF} = 1.3 \times V_s$$

The table below contains a list of common modern aircraft and the type of stall speed published for them by the manufacturer.

Aircraft	Stall Speed Certification Method
A300 Family	V_s
A320 Family	V_{s1g}
A330 Family	V_{s1g}
A340 Family	V_{s1g}
A350 Family	V_{s1g}
B737NG Family	V_{s1g}
B737MAX Family	V_{s1g}
B747-400	V_s
B757-200	V_s
B757-300	V_{s1g}
B767 Family	V_{s1g}
B777 Family	V_{s1g}
B787 Family	V_{s1g}
E170/190 Family	V_{s1g}

Table 1 Type of stall speed published for popular aircraft types [5] [6] [7].

From the approach reference speed V_{REF} , most Flight Management Systems will compute a target approach speed V_{APP} that is equal to $V_{REF} + 5 \text{ kt}$. From this baseline value of V_{APP} calculated by the FMS, pilots are typically trained to add an additional margin to the approach speed based on weather conditions expected on approach. Boeing suggests that pilots add half the expected headwind and all of the gust, for example. Airbus, on the other hand, suggests adding one-third of the headwind, and leaves any gust additive to pilot's discretion [8]. In the end, when observing the approach speeds of landing aircraft, we expect them to be flying at an indicated airspeed that corresponds to $V_{REF} + 5 \text{ kt} + \text{Wind Additive}$.

Because V_{REF} is correlated with stall speed (V_{s1g} or V_s), and stall speed is correlated with weight, our goal is to determine the relationship between weight and approach speed. Once this relationship is known, the observed airspeed on final approach can be propagated back to an estimate of the aircraft's landing weight. Since surveillance data reports the groundspeed of aircraft, converting this value to estimated indicated airspeed using the airport wind is an important step. Figure 4 below shows approaches made by Airbus A320 aircraft, highlighting the indicated airspeed on final approach. The data used is from an FDR dataset containing 240 Airbus A320 flights.

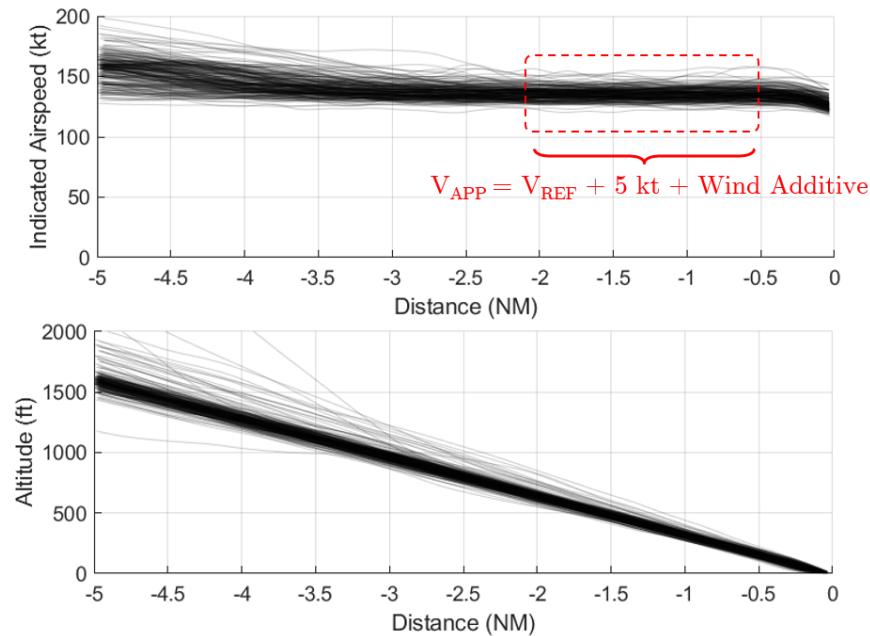


Fig. 4 FDR data for 240 A320 landings, showing the concentration of indicated airspeed values around typical landing speeds for this aircraft.

The flights in this dataset were operated on different days and landed at seven different European airports (EGLL, LFPG, LSZH, LFSB, LEMD, EBBR, and LIRF). The relationship between landing weight and approach speed (V_{APP}) for these flights can be viewed in Figure 5. Note that the weight values were available in the FDR dataset.

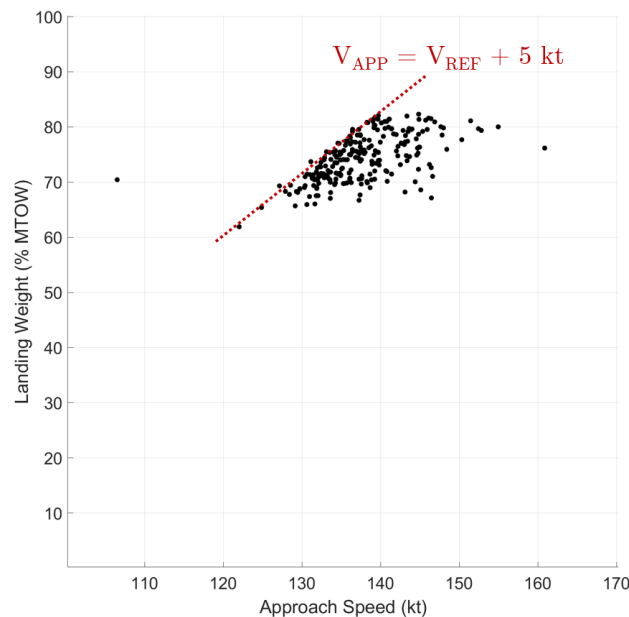


Fig. 5 Scatter plot of landing weights as a function of approach speed. The red line is the hypothetical baseline approach speed of $V_{REF} + 5 \text{ kt}$.

It can be seen in Figure 5 that approach speed values have a visible lower bound at each weight value, determined by the baseline approach speed computed by the FMS ($V_{REF} + 5 \text{ kt}$). This baseline speed is shown as the red dotted line. Approach speed values to the right of this line represent landings in which an additional margin was added to the final

approach speed (i.e. the *Wind Additive*). By evaluating the distribution of final approach speeds in this FDR dataset, the average wind additive was found to be 2 kt. Using this fact, V_{APP} becomes $V_{REF} + 7 \text{ kt}$ for the average case. Using the fact that the A320 uses V_{s1g} as its published stall speed (Table 1), the V_{APP} can be expressed in terms of the stall speed V_{s1g} as follows:

$$V_{APP} = 1.23 \times V_{s1g} + 7 \text{ kt}$$

From Figure 4, it is observed that the airspeed on final approach is the most stable between 1 NM and 2 NM from the runway. For the purposes of the weight estimation model, we therefore assert that the target V_{APP} equals the average airspeed observed within these two distance values. The stall speed V_{s1g} in the expression above can be written as a function of the aircraft's maximum lift coefficient $C_{L,max}$ and its landing weight W as follows:

$$V_{s1g} = \sqrt{\frac{2W}{\rho S C_{L,max}}},$$

where ρ is the air density and S is the aircraft's planform surface area. Using this, we can rewrite the expression for V_{APP} as follows:

$$V_{APP} = 1.23 \times \sqrt{\frac{2W}{\rho S C_{L,max}}} + 7 \text{ kt}$$

Solving for the landing weight W , we have:

$$W = \left(\frac{V_{APP} - 7 \text{ kt}}{1.23} \right)^2 \times \frac{\rho S C_{L,max}}{2}$$

This function can then be used to estimate the landing weight of aircraft in the FDR dataset and compare the results with their actual weights. For this, we use V_{APP} measured between 1 NM and 2 NM, ρ measured on the ground, and S and $C_{L,max}$ values obtained from BADA 4 for a full flap configuration. The results of the comparison are shown in Figure 6.

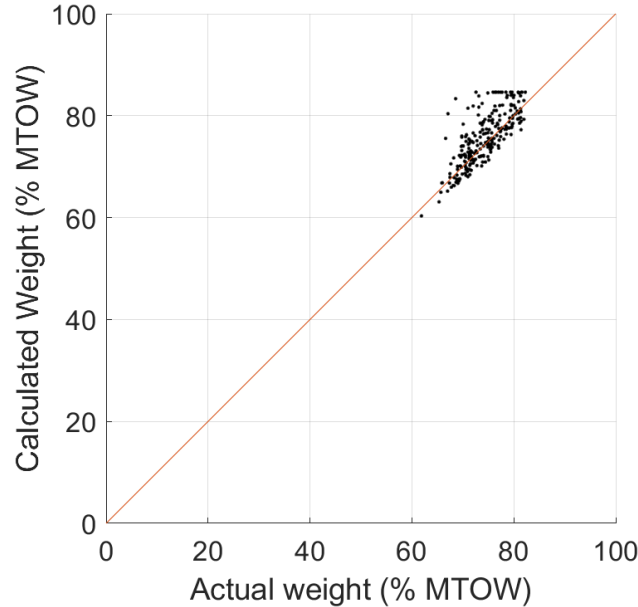


Fig. 6 Comparison of estimated landing weight values (y-axis) and actual FDR landing weight values (x-axis).

Figure 6 shows that the method outlined above is capable of producing reasonably accurate weight estimates. It should be noted that estimated weight values (y-axis) are constrained by the Maximum Landing Weight for the aircraft type in question. Figure 7 shows the distribution of weight estimate errors derived from the plot above. The longer tail on the right side of the distribution is indicative of flights that had a higher-than-average wind correction added to their

final approach speeds, while the left side of the distribution is expected to be bounded by the baseline approach speed of $V_{REF} + 5 \text{ kt}$.

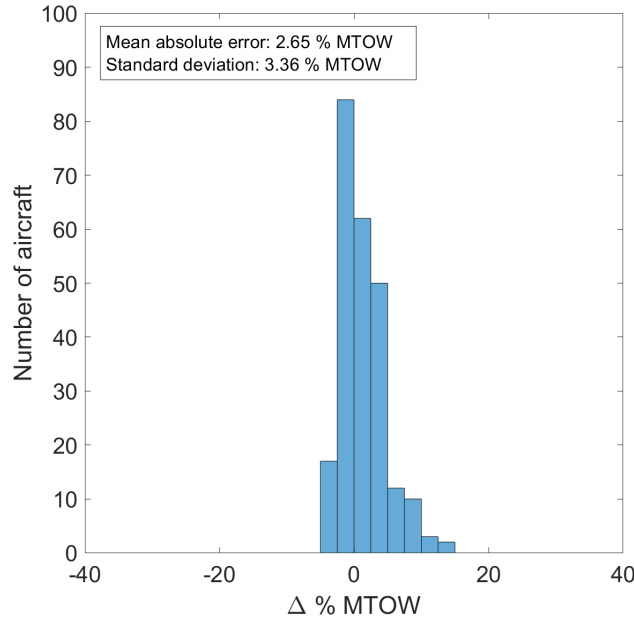


Fig. 7 Histogram of weight estimate errors measured in percentage of Maximum Takeoff Weight (MTOW).

This model was tested with four aircraft types for which FDR data was available, and the results can be seen in Table 2. When applying it to a surveillance dataset, accuracy will be improved when air density and local wind from additional sources can be used. Additionally, since surveillance data reports the groundspeed of aircraft, converting this value to estimated indicated airspeed using the airport wind is an important step. Finally, the user may also elect to change the value of the *Wind Additive* discussed earlier based on observed wind conditions, although a value of 2 kt was found to be a representative average. Different techniques for determining the *Wind Additive* are offered by different aircraft manufacturers [8], with the most common technique consisting of adding 1 kt to the approach speed for every 2 kt of headwind.

Aircraft	Number of Flights	Mean Absolute Error	Standard Deviation of Error
Airbus A319	191	3.63% of MTOW	4.02% of MTOW
Airbus A320	240	2.65% of MTOW	3.36% of MTOW
Airbus A321	176	3.75% of MTOW	3.45% of MTOW
Airbus A330-300	221	3.45% of MTOW	2.48% of MTOW

Table 2 Error statistics for landing weight estimation based on approach speed.

V. Takeoff Weight Estimation

In this section, a model is derived for estimating the takeoff weight of an aircraft based on airspeed and altitude measurements from the initial climb. To better expand on the method of estimation, a discussion of aircraft climb performance is warranted.

Most modern Flight Management Systems (FMS) plan climbs at a thrust value known as Maximum Climb/Continuous Thrust (MCT) [9]. In other words, climbs are performed at target airspeed values (e.g. 250 kts below 10,000 ft) and using a constant power setting (although maximum thrust decreases as altitude increases). For instance, on Airbus aircraft, MCT is the power setting maintained until cruise altitude is reached. While keeping the engines at MCT, the Flight Management System controls the aircraft pitch angle in order to maintain 250 KIAS below 10,000 ft, 300 KIAS above 10,000 ft, and Mach 0.78 above the IAS/Mach crossover altitude. At a constant power setting, the net thrust produced by the engines during climb is primarily a function of the Engine Pressure Ratio (EPR), which in turn is a function of Pressure Altitude and Total Air Temperature [10].

Referring to the same A320 Flight Data Recorder (FDR) data set discussed in the *Landing Weight Estimation* section, the variability of thrust as a function of distance from the runway during initial climb can be visualized in Figure 8, which shows data for 240 Airbus A320 departures.

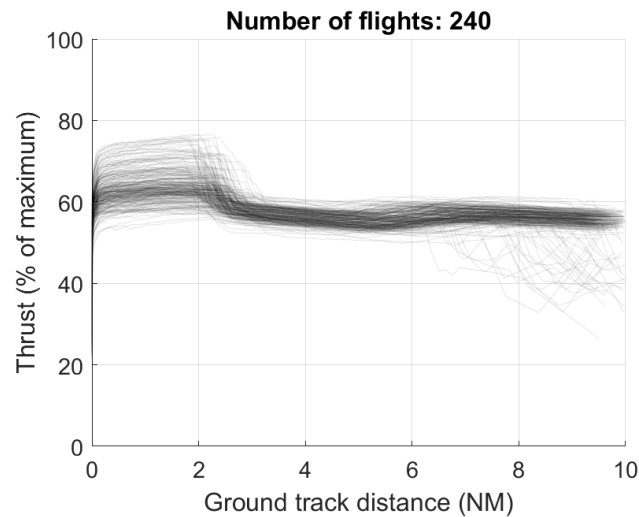


Fig. 8 Thrust as a function of distance from arrival end of runway for 240 A320 departures, as captured in Flight Data Recorder (FDR) data.

The data shown in Figure 8 depicts A320 aircraft departing from seven different European airports (EGLL, LFPG, LSZH, LFSB, LEMD, EBBR, and LIRF), with starting ground elevations ranging from sea level (LIRF) to 2000 ft (LEMD). The climb thrust values are observed to be reasonably concentrated after takeoff. The graphs in Figure 9 show how the climb thrust measured at a distance of 4 NM correlate with aircraft takeoff weight, pressure altitude, and airport air temperature at that same distance.

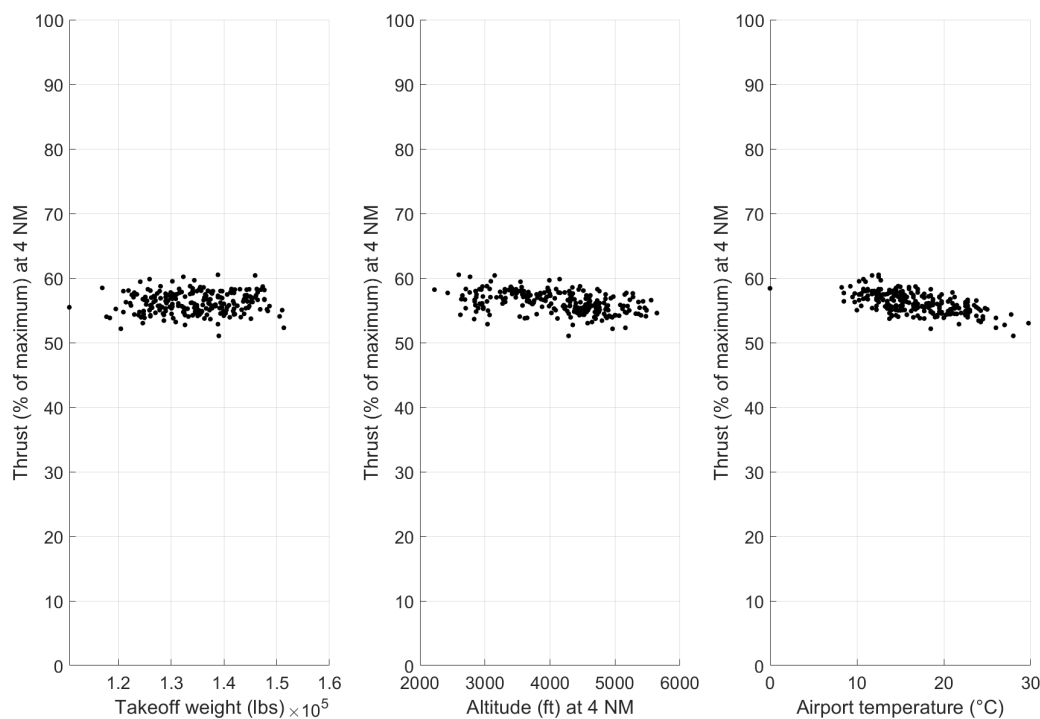


Fig. 9 Left: thrust recorded at a distance of 4 NM as a function of aircraft takeoff weight. Center: thrust recorded at a distance of 4 NM as a function of altitude at 4 NM. Right: thrust recorded at a distance of 4 NM as a function of airport air temperature.

It can be seen that climb thrust shows little to no correlation with takeoff weight, a slight negative correlation with altitude, and a moderate negative correlation with temperature. 95% of climb thrust values are recorded in the range between 53% and 59% of maximum thrust. Takeoff thrust (distance < 2 NM) shows considerable more variation, as expected due to the use of derated takeoff techniques at airports with longer runways, hotter temperatures, and/or when the aircraft is lighter. Derated takeoff procedures are commonly used to extend the operational lifespan of aircraft engines. Furthermore, the thrust of a few aircraft is observed to "dip" at distances beyond 6 NM. These events likely capture air traffic control restrictions that may enforce either a speed restriction or an altitude restriction on the flight, therefore causing the required thrust to decrease momentarily.

Based on the observation that differences in climb thrust among aircraft of the same type are relatively small, it stands that the climb performance of a given aircraft type should depend primarily on takeoff weight, with airport elevation and temperature being secondary factors. In other words, a heavier aircraft will climb slower than a lighter aircraft of the same type, since climb thrusts are expected to be similar based on the discussion above. Elevation and weather effects will also become less important when comparing departures at the same airport and under similar weather conditions. Appendix A shows the overall statistics for the climb thrust of additional aircraft for which Flight Data Recorder data was available.

Plotting the true airspeed, altitude and specific energy ($V^2 + gh$) for the 240 A320 departures shown in Figure 8, the differences in aircraft climb profiles due to variations in weight can be visualized (Figure 10).

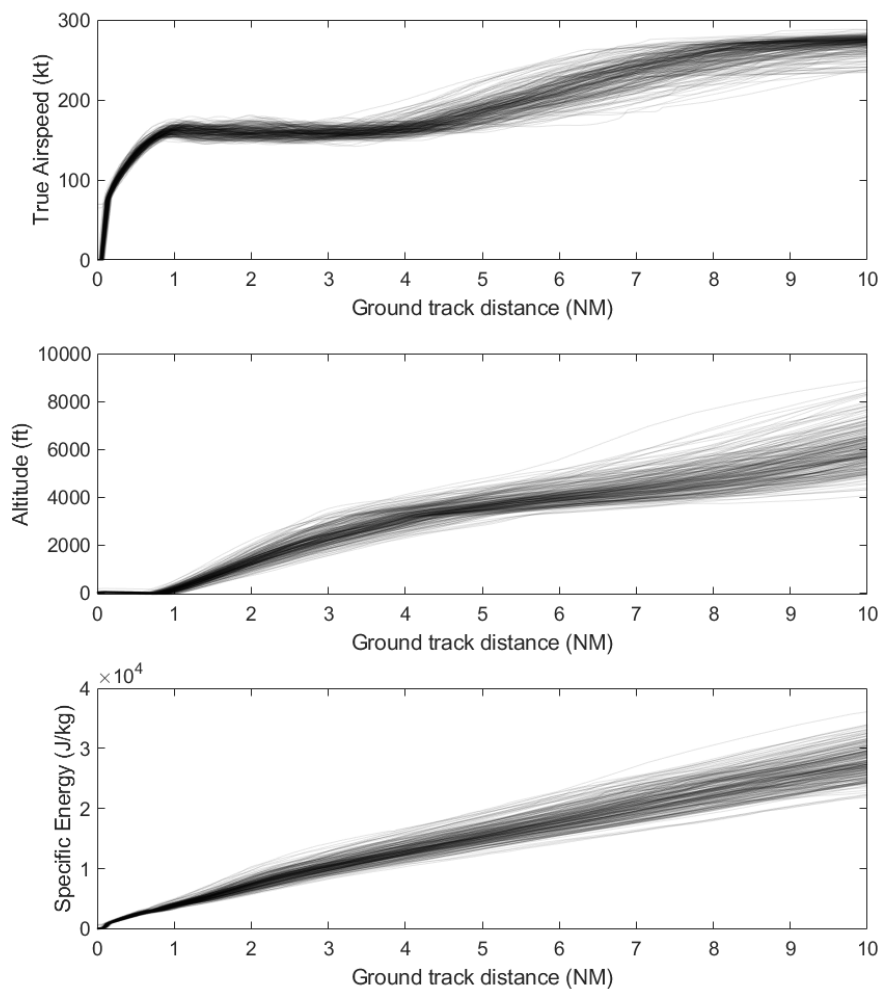


Fig. 10 True airspeed, altitude and specific energy as a function of distance for 240 A320 departures, as captured in Flight Data Recorder (FDR) data.

In the first 10 NM following takeoff, each aircraft climb profile depicts acceleration to initial climb speed (typically a value around $V_2 + 15$ kt), thrust reduction from takeoff to climb thrust, flap retraction, and subsequent acceleration to 250 KIAS. The rate of specific energy gain, which can be measured from the third plot in Figure 10, is therefore dependent on takeoff weight and, to a certain extent, on the timeline of gear and flap retraction. By looking at the total specific energy of each aircraft after enough time has elapsed for the aircraft to reach a steady-state climb, we can better isolate the effect of weight on the total energy. In other words, looking at the total specific energy at a distance of 10 NM, for example, is analogous to integrating the rate of specific energy gain for the first 10 NM of each flight and should correlate directly with the takeoff weight of each aircraft. Figure 11 plots takeoff weight and specific energy at 10 NM in the same graph, and a reasonable linear relationship between the two can be observed.

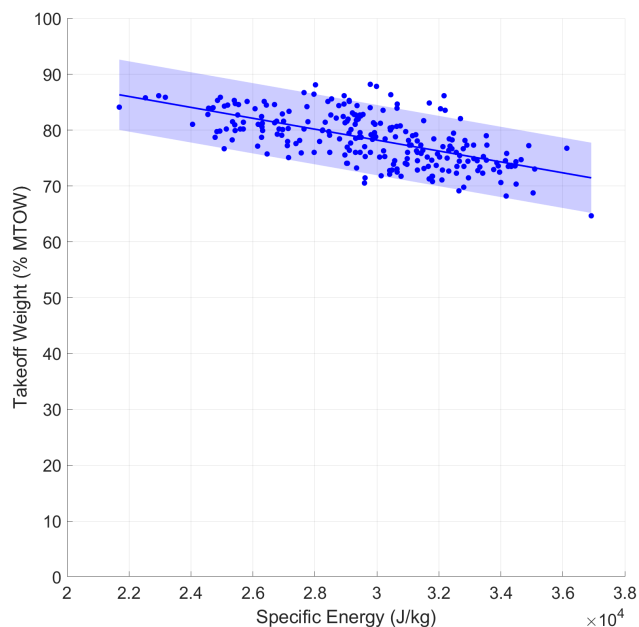


Fig. 11 Linear fit for the correlation between takeoff weight and specific energy measured at 10 NM. The dots represent actual aircraft weight from FDR, the line represents the best linear fit, and the shaded region represents the 95% confidence interval of the linear model.

In Figure 11, the dots represent actual aircraft weight values from FDR, the line represents the best linear fit, and the shaded region represents the 95% confidence interval of the linear model. The linear model performs reasonably well in estimating the takeoff weight. Because specific energy only requires basic aircraft states to be computed, namely airspeed and altitude, this linear model is proposed as a method to estimate takeoff weight from conventional surveillance data. Figures 12 and 13 illustrate the statistical performance of the sample model above as was done in the *Landing Weight Estimation* section.

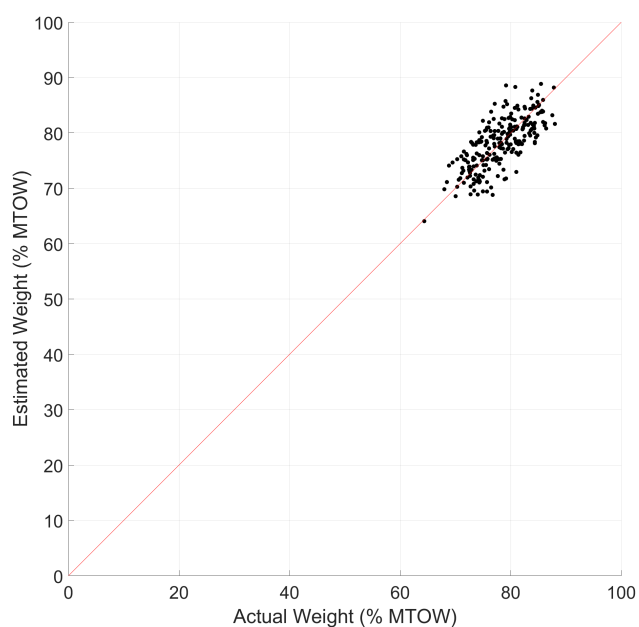


Fig. 12 Comparison of estimated takeoff weight values (y-axis) and actual FDR takeoff weight values (x-axis).

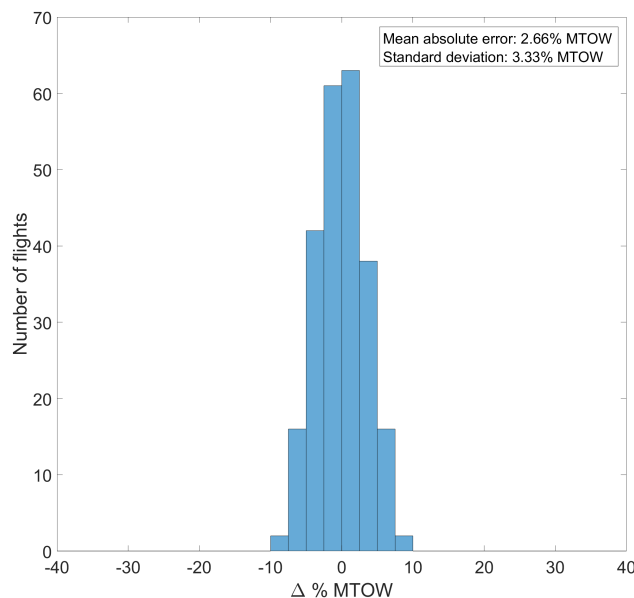


Fig. 13 Histogram of takeoff weight estimate errors measured in percentage of Maximum Takeoff Weight (MTOW)

At this stage, a reasonable linear relationship linking specific energy to takeoff weight has been derived for the Airbus A320 using FDR data. However, the parameters of this linear function are likely to change based on aircraft type. Since FDR data was not available for every aircraft type in this study, a general statistical method is still needed for estimation of takeoff weight of an arbitrary aircraft type when the only parameters available are airspeed and altitude (i.e. data from surveillance sources). The suggested strategy is described next.

First, given airspeed and altitude, specific energy values can be computed for all aircraft in a given surveillance dataset as $V^2 + gh$, where V is the airspeed in m/s , g is the gravitational acceleration in m/s^2 , and h is the altitude in meters. For a given aircraft type, values of specific energy at a distance of 10 NM from beginning of takeoff roll can be aggregated into a distribution. Figure 14 shows an illustration of this step applied to the Airbus A320. Results for other aircraft for which FDR data was available can be seen in Appendix B.

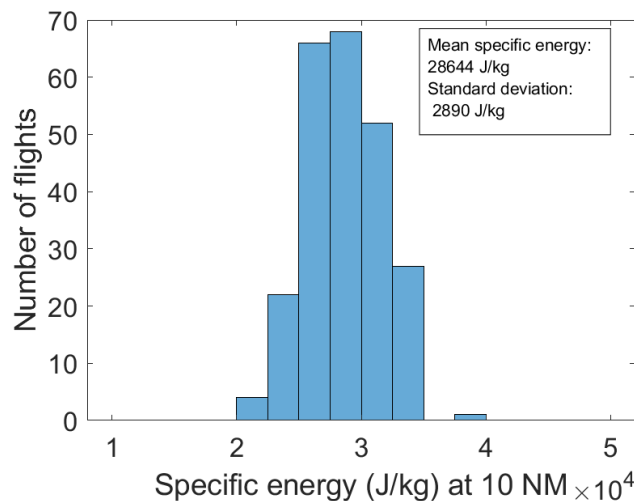


Fig. 14 Distribution of specific energy values recorded for the A320 (240 flights) at a distance of 10 NM.

Because of the assumption made that specific energy correlates linearly with takeoff weight, it stands that the mean value of the specific energy distribution corresponds to the mean value of the "hidden" takeoff weight distribution, while

the -1σ value of specific energy corresponds to the $+1\sigma$ value of takeoff weight. In other words, because of the linear assumption, an aircraft with an average specific energy value must also have an average takeoff weight value, while an aircraft with a specific energy value that is one standard deviation lower than average must have a takeoff weight that is one standard deviation higher than average (because of the negative slope in Figure 11). Therefore, given the observed distribution of specific energy values for a given aircraft type, individual aircraft takeoff weights can be estimated based on reasonable assumptions of the mean and standard deviation of the hidden takeoff weight distribution. While these two parameters may change based on aircraft type, departure airport, airline, and other variables, analysis of weight statistics for six aircraft types (Appendix C) shows that takeoff weight values typically average around 75% of MTOW, and have a typical standard deviation of about 5% of MTOW. Where knowledge of a typical weight distribution for the aircraft type in question is available, these parameters can be derived readily from such distribution. For the Airbus A320, the mean takeoff weight recorded in FDR data among 240 flights was 78.2% of MTOW, while the $+1\sigma$ value of takeoff weight was 82.7% of MTOW. Relating these two values to the mean and standard deviation of the specific energy distribution allows us to derive a linear fit function as shown in Figure 15.

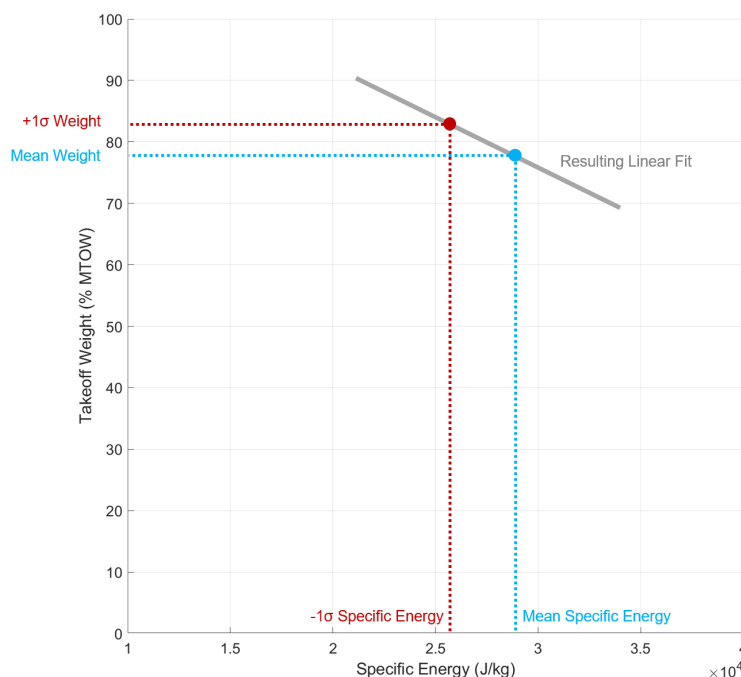


Fig. 15 Illustration of derivation of linear fit function relating specific energy to takeoff weight based on assumed values for the mean and the standard deviation of the hidden takeoff weight distribution.

Once this function has been determined for the aircraft type being analyzed, the weight of individual aircraft of the same type can be estimated by evaluating the linear fit at each aircraft's specific energy value. While it is acknowledged that the accuracy of this method is dependent on the assumptions made for the hidden takeoff weight distribution, it will still allow for a "correction" of takeoff weights in the expected direction by enforcing a correlation between observed climb performance and takeoff weight. This would not be the case, for example, if a simple mean weight assumption were applied to every aircraft in the dataset.

In order to minimize the effect of climb performance variations caused by changes in weather (ambient temperature and pressure) in the model, it is recommended that data from a relatively short time period (e.g. a week) be used to derive a linear fit for a given aircraft type. The derivation process can be repeated for each time period of interest for best accuracy, with each time period making use of its own linear function for weight estimation. However, if only a few aircraft of the type can be observed operating in each time period, the user may elect to increase the sample window in order to increase the number of observations. For the models derived in this study, the lowest number of samples used to derive a linear fit was 90 (Boeing 757-200), and the highest was 262 (A340-500).

Finally, it should be noted that the method described only applies to aircraft flying an unrestricted initial climb. Altitude restrictions may sometimes be imposed by air traffic control, and a proper specific energy value cannot be

calculated in this scenario. For aircraft observed flying restricted climbs, the user may therefore elect to simply use the mean takeoff weight as the assumed weight.

Table 3 below illustrates the accuracy of the method described in estimating the takeoff weight of various aircraft types. Note that, in these results, the mean and $+1\sigma$ takeoff weight values were derived directly from the FDR dataset.

Aircraft	Number of Flights	Mean Absolute Error	Standard Deviation of Error
Airbus A319	191	3.07% of MTOW	3.80% of MTOW
Airbus A320	240	2.66% of MTOW	3.33% of MTOW
Airbus A321	176	2.90% of MTOW	3.72% of MTOW
Airbus A330-300	221	2.62% of MTOW	4.32% of MTOW
Airbus A340-500	262	3.59% of MTOW	4.64% of MTOW
Boeing 757-200	90	3.42% of MTOW	4.56% of MTOW

Table 3 Error statistics for weight estimation based on linear fit of specific energy.

VI. Conclusion

This paper presented methods to estimate the takeoff and landing weight of large commercial aircraft based on basic aircraft states (i.e. airspeed and altitude). While the models are mathematically simple, they are based on standard aircraft operating procedures and should prove themselves robust. Weight estimation can be particularly useful in analyses requiring estimation of fuel burn and/or aircraft acoustic noise, where the estimation of thrust is dependent on weight.

Appendix A: Thrust Data Statistics from Flight Data Recorder

Aircraft	Number of Flights	-1σ Climb Thrust	Average Climb Thrust	$+1\sigma$ Climb Thrust
Airbus A319	191	60.0% Max Thrust	63.2% Max Thrust	66.5% Max Thrust
Airbus A320	240	54.6% Max Thrust	56.2% Max Thrust	57.8% Max Thrust
Airbus A321	176	50.9% Max Thrust	52.2% Max Thrust	53.5% Max Thrust
Airbus A330-300	221	41.8% Max Thrust	45.2% Max Thrust	48.5% Max Thrust
Airbus A340-500	262	37.3% Max Thrust	41.4% Max Thrust	45.6% Max Thrust
Boeing 757-200	90	44.4% Max Thrust	47.0% Max Thrust	49.7% Max Thrust

Table 4 Sample climb thrust statistics for all aircraft for which FDR data was available. Measured at 4 NM from beginning of takeoff roll.

Appendix B: Specific Energy Statistics at 10 NM from Flight Data Recorder

Aircraft	Number of Flights	-1σ Specific Energy	Average Specific Energy	$+1\sigma$ Specific Energy
Airbus A319	191	2.86×10^4 J/kg	3.13×10^4 J/kg	3.39×10^4 J/kg
Airbus A320	240	2.58×10^4 J/kg	2.86×10^4 J/kg	3.15×10^4 J/kg
Airbus A321	176	2.22×10^4 J/kg	2.55×10^4 J/kg	2.88×10^4 J/kg
Airbus A330-300	221	2.00×10^4 J/kg	2.35×10^4 J/kg	2.69×10^4 J/kg
Airbus A340-500	262	1.79×10^4 J/kg	2.14×10^4 J/kg	2.48×10^4 J/kg
Boeing 757-200	90	2.46×10^4 J/kg	2.78×10^4 J/kg	3.11×10^4 J/kg

Table 5 Sample specific energy statistics for all aircraft for which FDR data was available. Measured at 10 NM from beginning of takeoff roll.

Appendix C: Takeoff Weight Data Statistics from Flight Data Recorder

Aircraft	MTOW	Number of Flights	-1σ Takeoff Weight	Average Takeoff Weight	$+1\sigma$ Takeoff Weight
Airbus A319	166,000 lbs	191	71.7% MTOW	76.1% MTOW	80.6% MTOW
Airbus A320	172,000 lbs	240	73.7% MTOW	78.2% MTOW	82.7% MTOW
Airbus A321	206,000 lbs	176	68.8% MTOW	74.4% MTOW	80.0% MTOW
Airbus A330-300	533,519 lbs	221	70.0% MTOW	76.6% MTOW	83.1% MTOW
Airbus A340-500	840,000 lbs	262	64.3% MTOW	64.2% MTOW	74.2% MTOW
Boeing 757-200	255,000 lbs	90	74.4% MTOW	79.6% MTOW	84.9% MTOW

Table 6 Sample takeoff weight statistics for all aircraft for which FDR data was available.

Acknowledgments

This work was sponsored by the Federal Aviation Administration (FAA) under ASCENT Center of Excellence Project 23. Opinions, interpretations, conclusions, and recommendations are those of the authors and are not necessarily endorsed by the United States Government. The authors would like to acknowledge the support of Chris Dorian, Joseph DiPardo, and Bill He of the FAA Office of Environment and Energy.

References

- [1] Salgueiro, S., Thomas, J., Li, C., and Hansman, R. J., "Operational Noise Abatement through Control of Climb Profile on Departure," *AIAA Scitech 2021 Forum*, 2021.
- [2] Thomas, J., Mahseredjian, A., and Hansman, R. J., "Delayed Deceleration Approach Procedure Noise Modeling Validation using Noise Measurements and Radar Data," *AIAA Aviation 2021 Forum*, 2021.
- [3] Chati, Y. S., and Balakrishna, H., "Statistical Modeling of Aircraft Takeoff Weight," *Twelfth USA/Europe Air Traffic Management Research and Development Seminar (ATM 2017)*, 2017.
- [4] Airbus, *Getting to Grips with Aircraft Performance*, Jan. 2002.
- [5] Embraer, *Understanding Vref and Approach Speeds*, 2010.
- [6] Federal Aviation Administration, "Advisory Circular 25-7D - Flight Test Guide for Certification of Transport Category Airplanes," https://www.faa.gov/regulations_policies/advisory_circulars/index.cfm/go/document.information/documentID/1033309, 2018. [Online; accessed 24-May-2021].
- [7] FAA Airplane Performance Harmonization Working Group, "PERF HWG Report 4," https://www.faa.gov/regulations_policies/rulemaking/committees/documents/media/ACOapT1-11121997.pdf, 2002. [Online; accessed 24-May-2021].
- [8] Code 7700, "Approach Speed Wind Additives," https://code7700.com/approach_speed_wind_additives.htm, 2020. [Online; accessed 24-May-2021].
- [9] GE Aviation, "FAA CLEEN II - Flight Management System Final Report – Public Version," , Jan. 2020.
- [10] Airbus, *A319/A320/A321 Flight Crew Operating Manual*, 2002. Rev 35.